Tribology International 91 (2015) 160–169

Contents lists available at ScienceDirect

Tribology International

journal homepage: www.elsevier.com/locate/triboint

Fatigue damage mechanism of railway wheels under lateral forces

Guiyuan Zhou, Chenggang He, Guang Wen, Qiyue Liu *

Tribology Research Institute, State Key Laboratory of Traction Power, Southwest Jiaotong University, Chengdu, China

ARTICLE INFO

Article history:
Received 16 March 2015
Received in revised form
8 June 2015
Accepted 8 July 2015
Available online 17 July 2015

Keywords:
RCF
Lateral force
Plastic deformation
Fatigue cracks

ABSTRACT

Under conditions of curve negotiating and hunting, lateral force is generated at the wheel/rail interface that can damage the wheel tread. The rolling contact tests were performed on a JD-1 wheel/rail simulation apparatus with different lateral forces between the rail and wheel rollers. The results indicate that plastic deformation and mild wear dominated at each side of the contact area, while fatigue damage dominated at the middle region. Drastic changes in stress and stress direction from the high stress region to the lower stress region can lead to plastic accumulation and the initiation of fatigue cracks. The formation and breaking of metal tongue make big contribution to material loss in this condition.

1. Introduction

Increasing of the operation speed and axle load of a railway vehicle aggravate the issue of railway wheel damage in terms of safety and economy [1]. Wheels serve as a vital component of a vehicle, bearing the vertical load of the train and conveying the traction and braking forces between wheel and rail in severe operating conditions. Therefore, great emphasis has been placed on investigating the wear and fatigue mechanisms of railway wheels to improve the safety and economy of railway transportation [2–4].

Railway wheel damages reported by Bevan et al. [5] are classified into a number of categories, such as RCF, falts, ovality, cavities, tread wear and tread rollover, where RCF is most problematic mechanism caused wheel damage (41%). Many studies have reported that a wear mechanism can remove the material of the surface layer where RCF cracks nucleate; consequently, a competition mechanism between wear and RCF has been proposed [6–9]. Unlike the slow deterioration process of wear, RCF causes abrupt fractures in rims. Wear damages are visible and controllable, while RCF cracks are difficult to detect and potentially dangerous if not addressed. Usually, wheel fatigue failure modes are divided into three failure types that correspond with different initiation locations: surface, sub-surface and deep-surface [10,11]. With surface-initiated cracks, one of the damage mechanisms is called ratchetting [12,13] and typically occurs on the surface layers of wheels. The main causes of surface ratchetting are high friction loads that act parallel to the surface. Sub-surface cracks typically nucleate under the contact surface where the largest shear stress occurs or in the presence of structural inhomogeneities such as inclusions or defects [14]. Deep-surface initiated cracks are similar to sub-surface cracks but are located farther away from the contact point and may propagate in a low-stress field if the dimension is large enough.

Contact forces between wheel and rail are essential factors that determine the wear and RCF behaviors of the rim [15], and there are some methods to measure them [16,17]. RCF surface cracks usually occur due to unidirectional plastic material flow caused by tangential forces between wheel and rail. The forces experienced by the wheel bearing become complicated when the wheel is operated on curving tracks and can be broken down into three components: vertical, lateral and longitudinal [18]. Specially, the lateral force may lead to damages, such as tread rollover [19,20] (Fig. 1) due to plastic material flow, which follows the direction of tangential stress [21]. This will affect the comfort and safety of the ride and can also increase maintenance expenses.

Some researches on RCF have indicated that RCF cracks initiated in the contact surface [6,13,22], the lubrication such as water and oil may accelerate the propagation of fatigue cracks [23–26] which is one the main damage mechanisms occurring at wheels. In general, surface-initiated RCF depends on a number of interdependent parameters, such as the load [15], the slip ratio [27,28], the contact condition [29], the friction coefficient, the material defects [14], the wear and fatigue resistance of the material [30]. In practical cases, many factors affect the wear and fatigue behavior of the railway wheel, making it difficult to reliably quantify wheel and rail wear under a variety of operating conditions. So, the investigation of railway wheel damage caused by rolling contact relies heavily on experimental research.

* Correspondence to: Tribology Research Institute, State Key Laboratory of Traction Power, Southwest Jiaotong University, Chengdu 610031, Sichuan Province, P.R. China. Tel.: +86 28 87603724; fax: +86 28 87603142.
E-mail address: trilgmc@126.com (Q. Liu).

http://dx.doi.org/10.1016/j.triboint.2015.07.008
0301-679X/

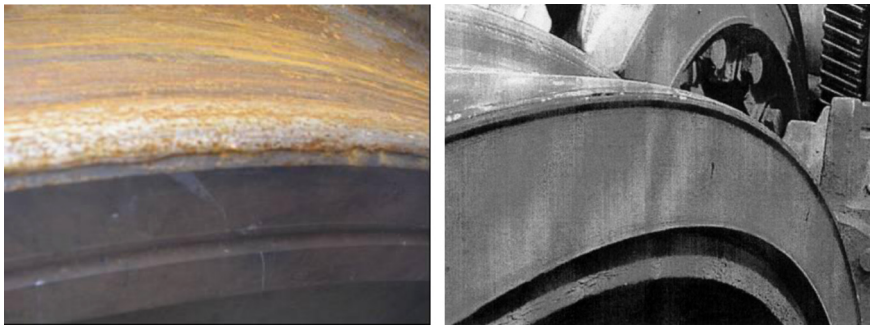

Fig. 1. Photograph of tread rollover [19,20].

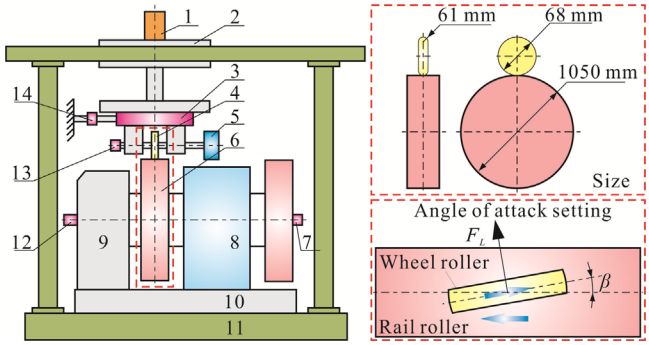

Fig. 2. The schematic, geometry and size of testing apparatus [31], 1 – Normal loading cylinder; 2 – Loading carriage; 3 – Vertical and longitudinal force collection unit; 4 – Wheel roller; 5 – Opposing torque unit; 6 – Rail roller; 7 – Revolution speed transducer; 8 – DC motor; 9 – Gear box; 10 – Turning plate; 11 – Base plate; 12 – Optical shaft encoder; 13 – Revolution speed transducer; 14 – Lateral force transducer.

This work conducted rolling contact tests using a JD-1 wheel/rail simulation apparatus with different lateral forces. We evaluated the wear behavior, the hardening effect of the contact surface and the relationship between lateral force and lateral plastic flow.

2. Experimental details

The schematic of JD-1 wheel/rail simulation apparatus [31] with minor modification is shown in Fig. 2. The apparatus is composed of a small wheel that served as the locomotive or rolling stock (called the "wheel roller") and a large wheel that served as the rail (called the "rail roller"). A DC motor drove the rail roller, and contact forces between rollers drove the wheel roller. Moreover, an opposing torque against the rotation direction was imposed on the axis of the wheel roller to generate a certain value of contact forces between wheel and rail rollers [30]. As the wheel roller is driven by contact forces, i.e. the rotational velocity cannot be directly controlled; therefore the creepage/slip was approximately controlled by setting the opposing torque. The longitudinal creepage for 4 specimens was estimated by measuring the rolling speeds and diameters of the wheel and rail rollers.

The vertical load was imposed by a hydraulic cylinder. The angle (β) between wheel and rail rollers which employed as the angle of attack, which was setting by rotating the turning plate relative to the base plate, as the position of rail roller is relatively fixed to the turning plate. The blue arrows denote the rolling direction of wheel and rail rollers, the wheel roller subjected a force at the contact area with axial direction which denoted as lateral force (F_L). An S-type force transducer with measurement uncertainty of 2% was employed to collect the lateral force between rollers during the rolling contact tests.

The geometric sizes of rollers are determined by means of the Hertzian simulation rule [1,31,32], i.e. both the maximum contact pressure and the ratio of the semi-major axis to the semi-minor axis of the contact path in the experimental condition is same as that in the practical, which is shown in Eqs. (1) and (2)

$$(P_{\max})_{\text{field}} = (P_{\max})_{\text{lab}} \tag{1}$$

$$(m/n)_{\text{field}} = (m/n)_{\text{lab}} \tag{2}$$

where $(P_{\max})_{\text{field}}$ and $(P_{\max})_{\text{lab}}$ are the maximum contact stresses in the laboratory and in the field, respectively; and $(m/n)_{\text{field}}$ and $(m/n)_{\text{lab}}$ are the ratios of the semi-major axis to the semi-minor axis of the contact ellipses between the wheel and rail in the laboratory and in the field, respectively.

The wheel rollers were extracted from the rim of the railway wheels and the rail roller was forged with U71M rail steel under the same heat treatment as real rails. The chemical compositions in weight percentage and the main mechanical properties of the rail and wheel materials are given in Table 1, where σ_b is the tensile strength; δ is the elongation; and ψ is the percentage reduction of area.

The rolling contact tests were performed at ambient room temperature without any lubrication between the rail and wheel rollers. In practical operations, when train speed reaches 250 km/h, the curve radius should be at least 7000 m; however, with a large curve radius, the corresponding angle of attack is very small, which is a disadvantage for the tests. Thus, severe curve radii were adopted to achieve good comparability. Table 2 displays the main parameters employed in the tests, other parameters are same for all specimens, setting the rolling speed of rail roller 69 rpm to simulate the speed of 250 km/h, the vertical load of 1392.5 N was employed to simulate the axle load of 19 ton, the total cycles of wheel rollers are 1×10^6, the opposing torque applied on the axis of wheel roller is 2.5 Nm.

The lateral forces during the rolling tests are also shown in Table 2, which indicate that a very small change in attack angle has a great influence on the value of the lateral force. Lateral force increases nonlinearly and gradually becomes saturated as the attack angle is increased; this corresponds with the results of Ishida et al. [33]. The friction coefficient of the specimens is 0.058, 0.154, 0.196 and 0.201 for specimens from #1 to #4 respectively, which has been estimated base on the force measurement.

Specimens were cleaned ultrasonically in ethanol prior to testing. Wear was measured through the mass loss by weighting the rollers before and after each test using an electronic balance with a resolution of 0.001 g (JA4103, China). The profile measurement was performed on each specimen before and after each test with a surface profilometer (JB-6C, China). The hardness of the surface in axial direction and subsurface in radial direction of the specimens were measured after the test by a Vickers hardness tester (MVK-H21, Japan), and the measure load is 4.9 N. Metallographic preparation